Supplemental Data

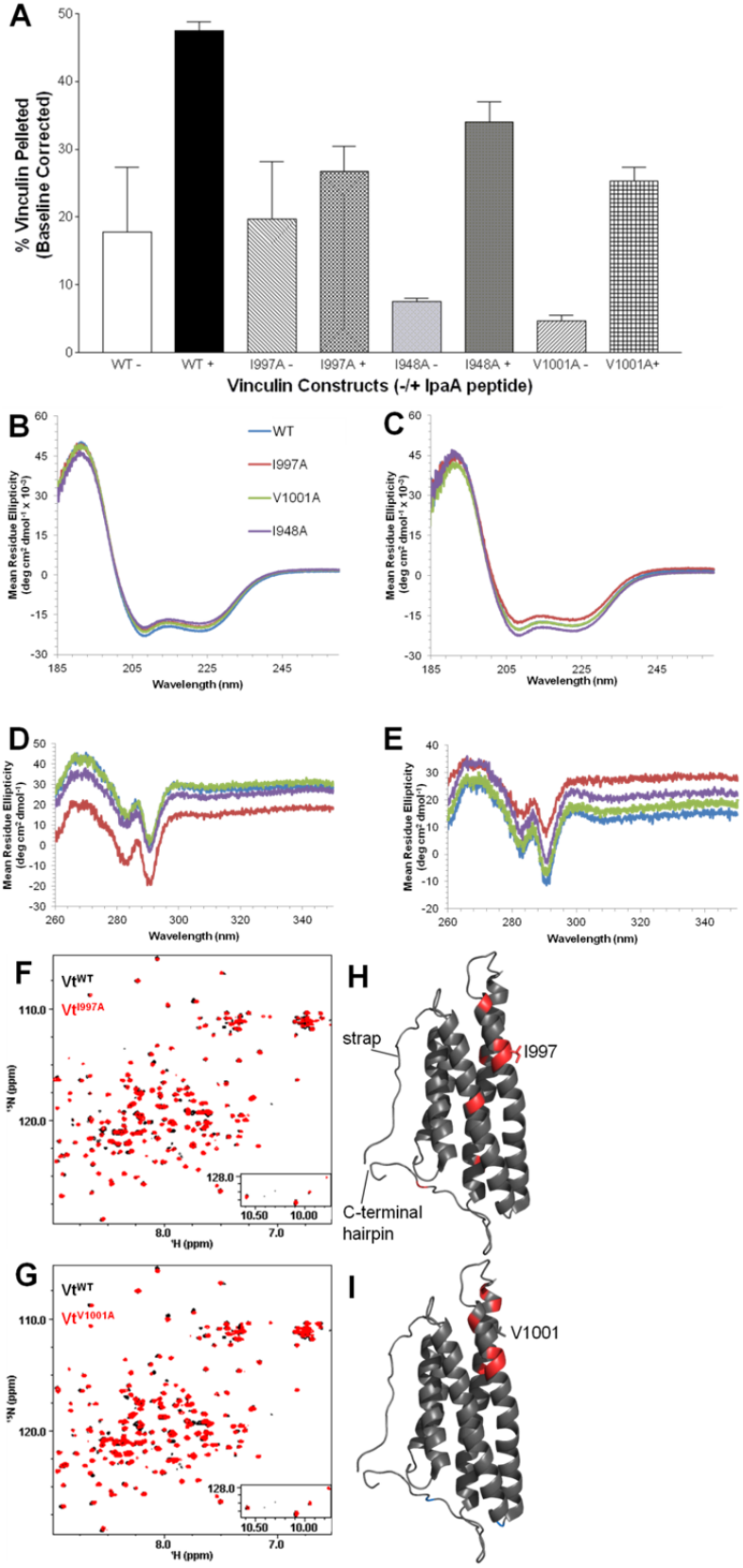

Figure S1. Further characterization of actin-binding deficient Vt variants (related to Figure 1). (A) Binding of F-actin by full-length vinculin^{WT}, vinculin^{I997A}, and vinculin^{I948A}. The percentage of vinculin bound to F-actin (30 μM) is shown, with

(+) and without (-) IpaA peptide. Addition of IpaA peptide disrupts autoinhibitory Vh:Vt interactions, exposing the actin-binding site on Vt and allowing it to bind with higher affinity to F-actin. Vinculin^{I997A} and vinculin^{V1001A} show significantly reduced F-actin association compared to vinculin^{WT} in the presence of the activating peptide. Vinculin^{I948A} binds to F-actin similarly to vinculin^{WT}. In the absence of the IpaA peptide, vinculin and its variants bind very little F-actin. Error bars are standard error. (B, C) Far-UV spectra of Vt^{WT} and variants Vt^{I997A}, Vt^{V1001A}, and Vt^{I948A} at pH 5.5 (B) and 7.5 (C). All three variants show similar α-helical content to Vt^{WT}. (D, E) Near-UV spectra of Vt^{WT} and Vt variants at pH 5.5 (D) and 7.5 (E). All Vt proteins exhibit similar spectra showing a distinct pattern between 260 and 300 nm, indicative of tryptophan packing interactions, suggesting that packing interactions between the N-terminal strap and C-terminal arm are retained. (F, G) ^{1}H-^{15}N HSQC of (F) Vt^{I997A} and (G) Vt^{V1001A}. The similarity of the overlaid spectra suggests that the chemical environment of the backbone amides remains largely unchanged. Downfield-shifted peaks are shown in the inset. (H, I) Peaks with significant changes in Vt^{I997A} and Vt^{V1001A}, respectively, are mapped onto the Vt^{WT} structure. Peaks with significant change in chemical shift (δ ppm > line width) are mapped on the structure in red, while those that exhibit significant broadening (line width > 2*linewidth^{WT}) are mapped in cyan. Residues that significantly shift in Vt^{I997A} are K956, K996, I997, L998, T1004, V1024, E1040, and V1059. Residues that significantly shift in Vt^{V1001A} are K996, I997, L998, A1003, D1013, E1015, and H1025. The side chain associated with the mutation site is shown in sticks. Residues that shift significantly are close to the site of mutation, suggesting that the perturbations are localized.

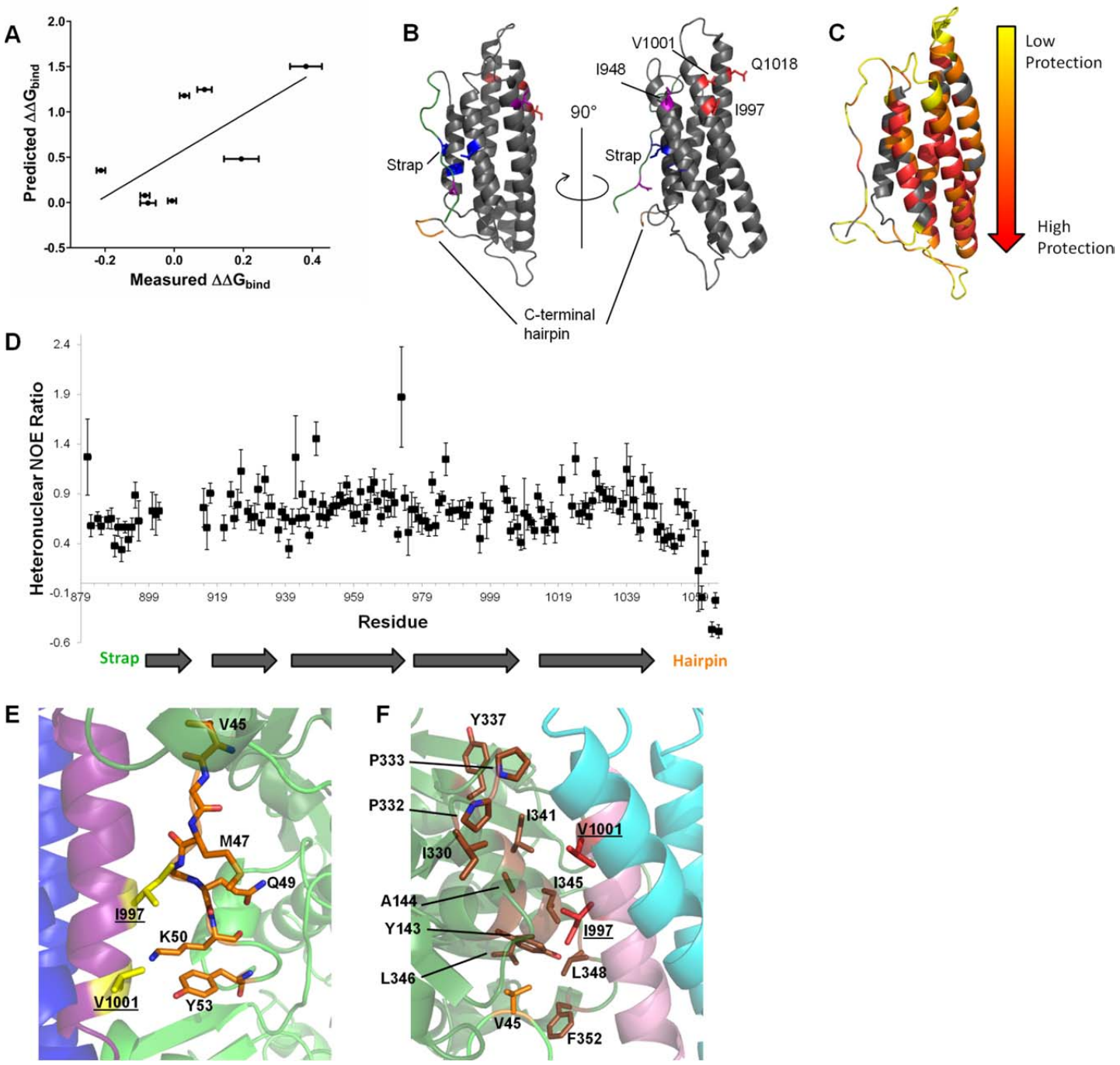

Figure S2. Evaluation of the DMD model (related to Figure 4). (A) Evaluation of the Vt-actin DMD model. The change in free energy of binding for Vt^{WT} and Vt variants (10 μM) with F-actin (30 μM) compared with values obtained using Eris (Ding et al., 2008; Yin et al., 2007a; Yin et al., 2007b) (Table S1). The DMD model shows a reasonable fit to the data (R^2 = 0.467, p-value for non-zero slope of 0.62). The fit is not as strong if data for I997A is not included (not shown, R^2 = 0.202, p-value of 0.31). (B) The Vt variants from Table S1 are mapped onto the Vt structure (PDB 1ST6). Residues in red, when mutated, decrease the affinity for F-actin. Residues in purple have no significant effect on actin binding to Vt, and residues in blue, when mutated, increase the affinity for F-actin. The N-terminal strap is in green and the C-terminal hairpin in

orange. (C) Protection factors from hydrogen exchange NMR experiments. Residues are colored based upon their protection factors. Residues in red exhibited the greatest protection, with residues in yellow the least. Residues in orange fall in the middle of the spectrum. Residues in gray are not assigned. (D) Heteronuclear NOE NMR spectroscopy data. The graph displays the ^{15}N heteronuclear NOE ratio at 60.78 MHz for Vt^{Q1018K}. Values near 0.8 are indicative of greater rigidity, while lower values indicate greater motion on the ps-ns timescale for the backbone amides. Error bars reflect experimental error. The arrows represent Vt helices, with the N-terminal strap and C-terminal hairpin labeled. These data reveal that in Vt^{Q1018K}, and likely Vt^{WT}, the N-terminal strap and especially the C-terminal hairpin are conformationally mobile. (E) Enlarged view of the Vt:F-actin interface from the manual fit model. The color scheme is maintained from Fig. 4. Vt is in blue, with H4 in purple. I997 and V1001 are shown in yellow with side chains represented as sticks and underlined. The actin residues near I997 and V1001 are shown in orange sticks and are labeled, and are located on the barbed end actin protomer. (F) Enlarged view of the Vt:F-actin interface from the DMD model. The color scheme is maintained from Fig. 4. Vt is in cyan, with H4 in pink. I997 and V1001 are shown in red with side chains represented as sticks and underlined. The side chains of nearby hydrophobic actin residues are labeled shown as sticks. The residues belonging to the pointed end actin protomer are shown in brown, with the residues belonging to the barbed end protomer shown in orange. Of the labeled actin residues, only V45 belongs to the barbed end protomer. These actin residues are located in a hydrophobic cleft previously identified as a common binding site for many actin-binding proteins (Dominguez, 2004). (E) and (F) provide additional details about the models but are not intended to identify specific residue-residue contacts between Vt and F-actin.